Synthesis and characterization of TiO_2 doped with Dy^{3+} ions by sol gel method.

M S Mokoena*, M Y A Yagoub, O M Ntwaeaborwa and H C Swart*
[1]Department of Physics, University of the Free State, Bloemfontein, ZA9300, South Africa

*Corresponding authors e-mail: swarthc@ufs.ac.za, mokoenams@ufs.ac.za

Abstract. Dy^{3+} ions doped in TiO_2 nanophosphor powders were synthesized by the sol-gel method. The prepared samples were characterized by X-ray diffraction (XRD), photoluminescence spectroscopy (PL), ultra-violet visible spectroscopy (UV-Vis), scanning electron microscopy (SEM) and energy dispersive x-ray spectroscopy. The XRD patterns confirmed the tetragonal structure of TiO_2 with the experimental unit cell parameters of a = b = 3.803Å and c = 9.534Å. The average crystallite sizes were estimated by applying the Debye-Scherrer formula and range from 9 to 5 nm. The FE-SEM images showed that the obtained powders surface texture was composed of nanorods. The EDS spectra confirmed the formation of undoped and doped TiO_2 nanophosphors. The UV-Vis diffuse reflectance spectra indicated the absorption bands in the visible region ranging from 460 to 850 nm which originated from the doped nanophosphors. The sharp absorption edge has shifted towards the longer wavelengths with the introduction of Dy^{3+} ions into the TiO_2. The optical band gap of the synthesized nanophosphor powder was determined and ranged from 3.41 to 3.06 eV. The emission bands of the Dy^{3+} ions were observed at 483, 576, 665 and 765 nm, which were assigned to different transitions of the 4f - 4f levels.

1. Introduction

Titanium dioxide is also known as titania or titanium oxide which has a chemical formula of TiO_2 and belongs to the IVB group transition metal oxides. Titania occurs in three common known polymorphs such as anatase (tetragonal), rutile (tetragonal) and brookite (orthorhombic). The above phases are differentiated from one another by their band gap energy and by also their refractive index (Eg = 3.2 eV, n = 2.488 for anatase, Eg = 3.0 eV, n = 2.608 for rutile and Eg = 1.96 eV, n = 2.583 for brookite). Furthermore TiO_2 has a low phonon frequency (<700 cm^{-1}) [1]. Generally the two polymorphs studied are the anatase phase and rutile phase [2]. In addition the rutile phase is considered to be the most stable phase especially at high temperature, while the anatase phase is stable at low temperatures.

Due to the unique properties, titania nanomaterial is considered to be one of the most important metal oxides in the past few years. Many researchers focus on titania due to the wide range of applications in solar cells, photocatalysts, cosmetics, lithium batteries, dye sensitized and chemical sensor and so forth [2, 3]. The applications of rutile and anatase phases will differ because of the different bonding arrangement [2].

Over the past few decades it has been noted that the properties of titania can be modified by doping TiO_2 with lanthanide ions. TiO_2 is one of the more favorable host materials for the incorporation of lanthanide ions due to its interesting properties such as friendly to the environment and its excellent chemical and thermal stabilities. Different researchers have synthesized TiO_2 nanoparticle doped with different lanthanide ions in the past years including TiO_2:Tb^{3+} [4, 5], TiO_2:Sm^{3+} [6, 7], TiO_2:Pr^{3+} [8] and

TiO_2:RE ions [9] for different applications. In addition the presence of rare earth ions in TiO_2 nanocrystalline stabilizes the anatase phase. The Dy^{3+} ion has been chosen to dope TiO_2 because of the fact that Dy^{3+} ions emit light at different ranges in the visible spectrum. There are several methods to synthesize TiO_2 nanoparticle but the focus was on the sol-gel method in this report because it is an inexpensive method and it requires lower temperatures.

The important goals of the present work was to synthesis the titanium oxide nanocrystalline powders by the sol-gel technique at room temperature and also to study the influence of the Dy^{3+} dopant on the structure and optical properties of TiO_2 nanocrystalline powder. The particle size and crystal structure of the synthesized samples were characterized using X-ray diffraction (XRD), surface morphology and chemical composition were determined using scanning electron microscopy (SEM) and energy dispersive x-ray spectroscopy (EDS), respectively, while the emission and excitation of the prepared samples were investigated by using photoluminescence spectroscopy (PL). In addition the optical indirect band gap energies of the prepared samples were obtained by using ultra-violet visible spectroscopy (UV-Vis).

2. Experimental Section

2.1 Synthesis

The undoped and doped TiO_2 nanophosphor powders were prepared by the sol-gel routine at room temperature by using Titanium butoxide (97%, Sigma Aldrich) as the precursor, Ethanol absolute (99.7%, associated chemical enterprise), and Acetic acid (≥ 99%, Sigma Aldrich) as the starting materials and dysprosium (iii) nitrate hydrate (99.9%, Sigma Aldrich) was used as a dopant ion.

Typically, the 25 mL of acetic acid was mixed together with 25 mL of ethanol in a 200 mL beaker and the mixture was stirred for 30 minutes using a magnetic stirrer to obtain the complete esterification solution. Afterwards, the 2.5 mL of titanium butoxide was added into the esterification solution to prepare the undoped nanophosphor. But for the doped nanophosphor a certain volume of titanium butoxide and different concentrations of $Dy(NO_3)_3.5H_2O$ were added simultaneously to the esterification solution. After the addition, the mixture was stirred continuously for an hour to form a sol at room temperature. The sol was aged for 24 hours at room temperature under the vacuum in order to form the white precipitation, and the white precipitations were dried in an oven for 30 minutes at 120°C. The pestle and mortar was used to grind the dried powder obtained from the oven. The grinded nano TiO_2 powder was then transferred into a muffle furnace and calcined at 400°C for 2 hours at a rate of $5°C.min^{-1}$.

2.2 Characterization Techniques

The crystallite size and phase of the TiO_2 nanophosphor for all synthesized samples were investigated using XRD patterns that were measured by a Bruker AXS D8 Advanced X-ray diffractometer with Cu $K\alpha = 1.5406$ Å radiation in the range $2\theta = 20 - 80°$ and a scanning rate of $0.02°.s^{-1}$.

The particle morphology and elemental composition of the prepared samples were studied using a Joel JSM-7800F Field Emission equipped with an Oxford Aztec EDS and a Gatan Mono CL4, which was used to identify the elements in the prepared samples. The samples were mounted on carbon tape during the analysis of SEM and EDS.

The optical properties of the synthesized nanophosphor powders were recorded in a scan range of 270 – 850 nm using an ultra violet visible spectrophotometer (Perkin Elmer UV/Vis Lambda 950 powder spectrophotometer) and using a lab-sphere for calibration and standard reference. Furthermore, both excitation and emission spectra of prepared samples were investigated with a Cary Eclipse fluorescent spectrometer using a Xenon lamp as excitation source. All the measurements were done at room temperature.

3. Results and Discussion

3.1 X-ray diffraction (XRD)

The XRD patterns of undoped TiO_2 nanophosphor powder and Dy^{3+} doped TiO_2 nanophosphor powders via sol-gel method are presented in Figure 1. The patterns indicate that the tetragonal phase of TiO_2 has formed and they were indexed according to the JCPDS card number 21-1272 (Anatatse) and JCPDS card number 21-1276 (Rutile). The undoped XRD patterns consisted of mixed phases of anatase and a minor content of rutile, while the doped patterns depict that Dy^{3+} ion prevented phase transformation of anatase-rutile by stabilizing only the anatase phase. The same phase was observed for all doped sample without any impurity which may relate to Dy_2O_3 or other phases of Dy in the XRD patterns and therefore this shows that Dy^{3+} ions were well incorporated into the TiO_2 host material.

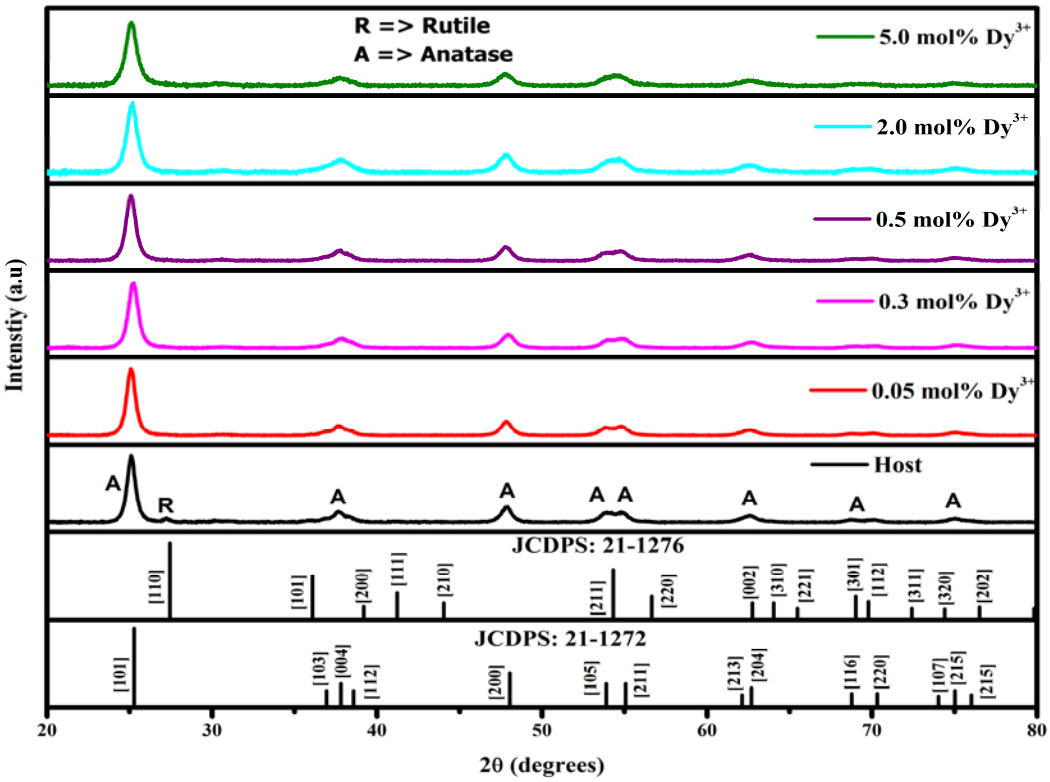

Figure 1: The XRD patterns of the TiO_2: Dy^{3+} nanophosphor powders. ("A" represent anatase phase and "R" represent the rutile phase).

It has been noted that the rutile phase is more stable especially at higher temperatures than the anatase and brookite phases [2], while the anatase phase can be stabilized by introducing dopants into the TiO_2 crystal structure. The XRD of the doped nanophosphor show no visible evidence of the rutile phase in Figure 1, centered at around 27.27°. Fidelus et.a1 [10] observed the same behavior when TiO_2 was co-doped with Nd^{3+} and Yb^{3+} ions and this effect indicates that the dopant retards the transition of TiO_2 from anatase to rutile phase, therefore stabilizing the anatase phase. The average crystallite sizes of Dy^{3+} doped TiO_2 nanophosphor with different doping concentration were estimated by applying the Debye-Scherrer formula [10, 11].

$$D = \frac{k\lambda}{\beta Cos\theta} \quad (1)$$

where k is constant k = 0.89 for spherical nanoparticles, λ is the wavelength X-ray radiation (Cu Kα=1.5406 Å), β is the full width at half maximum (FWHM) of the particular peak in radians and θ is the measured Bragg's angle in degrees. The average crystallite sizes ranged from 9 to 5 nm.

3.2 Scanning electron microscopy and energy dispersive x-ray spectroscopy.

The SEM images and EDS spectrum of synthesized nanophosphor powders are shown in Figure 2 and Figure 3 respectively. The shape morphology was obtained by using FE-SEM as shown in Figure 2 (a) and (b) for undoped TiO_2 and doped TiO_2 with 5.0 mol% of Dy^{3+} respectively. The figure shows that the surface texture was composed of nanorods for both the undoped and doped TiO_2 nanophosphor. This proves that the Dy^{3+} ion did not affect the particle morphology of the synthesized nanophosphors.

The EDS spectra confirm the presence of elements such as Ti, O, and C in the pure synthesized TiO_2 nanophosphor and the same elements in the doped TiO_2 nanophosphor, including the foreign element Dy ion. It thus confirmed that the pure anatase (TiO_2) was synthesized since no other elements where detected as shown in Figure 3 (a) beside Ti and O. The presence of carbon is from the carbon that was used to mount the sample during the analysis of SEM and EDS.

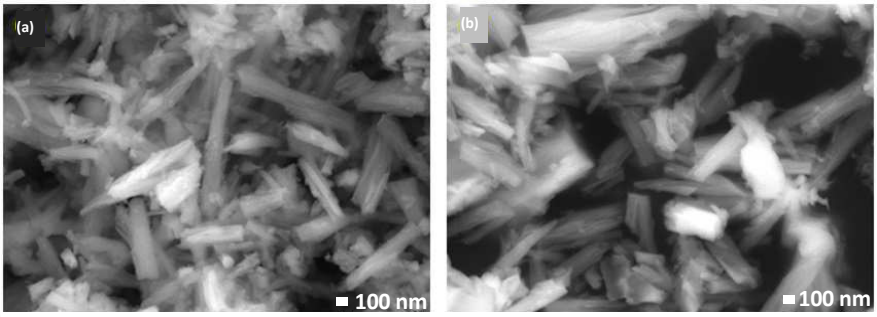

Figure 2: FE-SEM images of the (a) undoped and (b) 5.0 mol% Dy^{3+} doped TiO_2 nanophosphor powders.

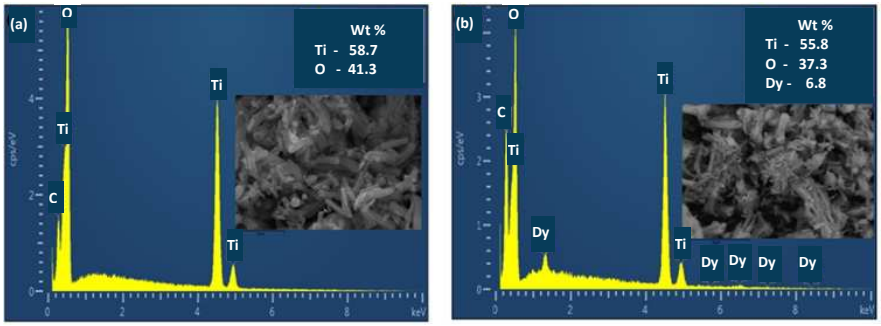

Figure 3: The EDS spectra of the undoped and 5.0 mol% Dy^{3+} doped TiO_2 nanophosphor powders.

3.3 Ultra-violet spectrophotometry

The absorption properties of the prepared samples were obtained from the diffuse reflectance spectra (DRS) as shown in Figure 4(a). It is clear that the absorption bands in a visible region (450 to 850 nm) originated from the doped samples, while for undoped sample there was no sign of absorption bands in that region. The absorption bands centered at 454, 475, 752 and 801 nm originated from the ground $^6H_{15/2}$ state to different excited states of the Dy^{3+} ion [12]. The sharp absorption edge was observed at ~ 365 nm for the undoped nanophosphor powder, but it shifts towards the longer wavelength after Dy^{3+} was introduced into the TiO_2 matrix. However, this absorption edge is assigned to the intrinsic absorption band of TiO_2. The optical band gap energy was also calculate by using the Kubelka-Munk remission function [11] and Figure 4 (b) was used to obtain the band gap values, which ranged from 3.41 to 3.06 eV.

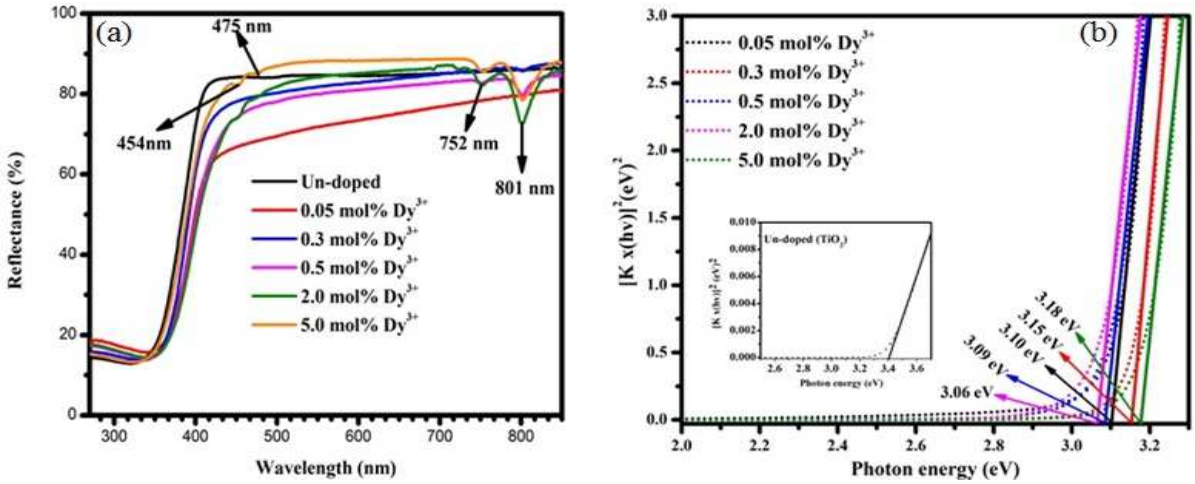

Figure 4: (a) DRS of Dy^{3+} doped TiO_2 nanophosphor and (b) Kubelka Munk transformed reflectance spectra of TiO_2 nanophosphor powders.

Figure 5 illustrates the excitation spectrum of pure TiO_2 nanophosphor and Dy^{3+} doped TiO_2 nanophosphor with different doping concentrations, monitored at an emission wavelength of 576 nm. There were four main excitation peaks with maxima at 392, 428, 453 and 474 nm which were assigned to electronic transition as shown in Figure 5.

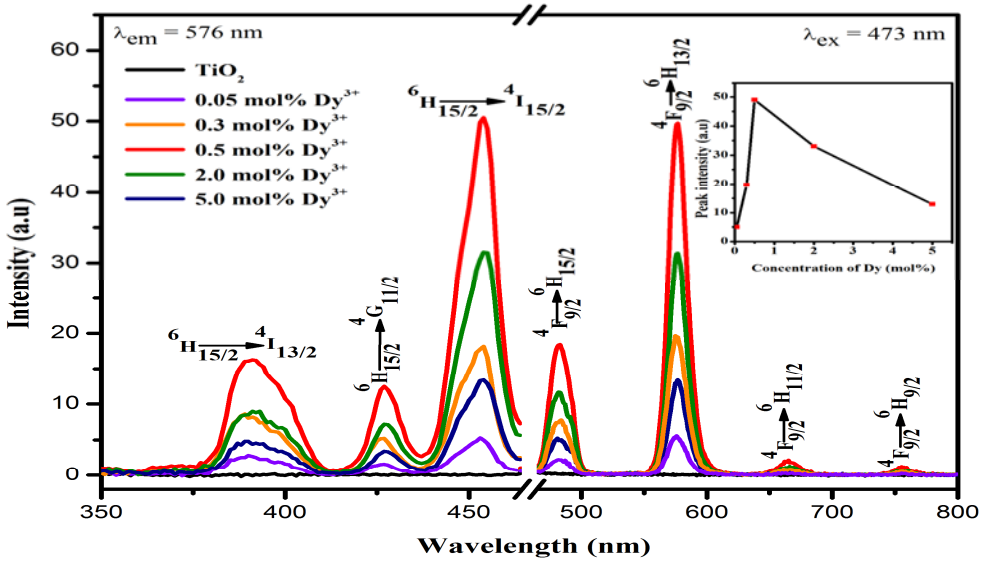

Figure 5: Excitation and emission spectra of Dy^{3+} doped TiO_2 nanophosphor with different doping concentration, (λ_{em} = 576 nm) and (λ_{ex} = 453 nm) respectively. (Inset shows the maximum emission intensity as function of Dy^{3+} concentration).

The emission spectra of Dy^{3+} doped TiO_2 nanophosphor with different doping concentration is also presented in Figure 5, under the excitation wavelength of 453 nm. The four main emission bands were observed with maxima at 483, 576, 665 and 765 nm, which were attributed to the transitions $^4F_{9/2} \rightarrow {}^6H_{15/2}$, $^4F_{9/2} \rightarrow {}^6H_{13/2}$, $^4F_{9/2} \rightarrow {}^6H_{11/2}$, $^4F_{9/2} \rightarrow {}^6H_{9/2}$ of Dy^{3+}, respectively [12]. The yellow emission centered at 576 nm has the most intense emission bands for all prepared samples. (The inset shows the intensity as function of Dy^{3+} concentration). The transition at wavelength centered at 576 nm (yellow) $^4F_{9/2} \rightarrow {}^6H_{13/2}$ belongs to the electric dipole transition, while the hypersensitive transition $^4F_{9/2} \rightarrow {}^6H_{15/2}$ at 476 nm band (blue) corresponds to the magnetic dipole of the Dy^{3+} ion.

4. Conclusion

A series of TiO_2 nanophosphor doped with Dy^{3+} were successfully synthesized by sol-gel method. The XRD patterns confirmed the tetragonal structure of TiO_2, although the XRD patterns of undoped nanophosphor consisted of a mixture of anatase and rutile. It was clearly shown that the Dy^{3+} ion played an important role in the crystal structure of TiO_2 because the presence of the Dy^{3+} ions stabilized the anatase phase. The average crystallite sizes were estimated to range from 7 to 9 nm for all samples. The EDS spectra confirmed that the synthesized nanophosphor was pure TiO_2 since no impurity elements were detected in the prepared nanophosphor material. The surface texture was composed of nanorods for pure TiO_2 and doped TiO_2 nanophosphors. The absorption bands in the visible range were observed by using UV-Vis diffuse reflectance spectroscopy. The optical indirect band gap energies of TiO_2 nanophosphor powders were estimated by using the diffuse reflectance spectra to plot the Kulbeka-Munk function for an indirect band gap. The estimated band gap energies ranged from 2.92 to 3.13 eV for the doped and undoped nanophosphors. The two major emission bands of Dy^{3+} ion were observed at 483 nm and 576 nm and the maximum emission intensity was obtained when the Dy^{3+} concentration was 0.5 mol%. It was noted that the luminescence intensity depended on the Dy^{3+} ion concentration.

Acknowledgements

This research is supported by the South African Research Chairs Initiative of the Department of Science and Technology and the National Research Foundation of South Africa (grant 84415). The financial support from the University of the Free State is also acknowledged.

5. References

[1] Brik M G, Anti Z M, Vukovi K, and Drami M D 2015 *Mater. Trans*. **56** 1416.
[2] Choudhury B and Choudhury A 2013 *Inter. Nano Lett.* **3** 55.
[3] Masuda Y and Kato K 2009 *J. Ceramic Soc Jap*. **117** 373.
[4] Wojcieszak D, Kaczmarek D, Domaradzki J, and Mazur M 2013 *Inter. J. Photoenergy* 2013 526140.
[5] Jia C, Xie E, Peng A, Jiang R, Ye F, Lin H, and T. Xu T 2006 *Thin Solid Films* **496**, 555.
[6] Kiisk V, Šavel M, Reedo V, Lukner A, and Sildos I 2009 *Phys. Proc*. **2**, 527.
[7] Reszczynska J, Esteban D A, and Gazda M 2014 *Fizykochemiczne Problemy Mineralurgii - Physicochemical Problems of Mineral Processing* **50** 515.
[8] Theivasanthi T and. Alagar M 2012 *Nano Biomed. Eng.* **4(2)** 58
[9] Bahadur N, Jian K, Pasricha R, Govind, Chand S 2011 *Sens. Actuators B Chem*. **159** 112.
[10] Ogugua S, Swart H C, and Ntwaeaborwa O M 2016 *Physica B* **480**, 131.
[11] Molefe F V, Koao L F, Dolo J J, and Dejene B F 2014 *Physica B* **439** 185.
[12] Vishwakarma A K, Jha K, Jayasimhadri M, Sivaiah B, Gahtori B, and Haranath D 2015 *Dalton Trans.* **44**, 17166.